Chronic cerebral hypoperfusion induces cerebral hemodynamics and angiogenesis

Shi Chang-Zheng[1], Jing Zhen[1], Ruan Yiwen[1], and Huang Li¡¯an[1]

[1]*Jinan University, Guangzhou, Guangdong, China*

Background and Purpose: Chronic cerebral hypoperfusion (CCH) induces cognitive impairment, but the compensative mechanism of cerebral blood flow (CBF) is not fully understood. To further reveal information on such mechanisms, the present study aimed to investigate dynamic changes in CBF and angiogenesis of CCH brains induced by bilateral common carotid artery occlusion (BCCAO) in rats.

Materials and Methods: Adult male Wistar rats(n = 40) were used to establish the experimental models. The right common carotid artery (RCCA) was carefully separated from the adjacent vagus nerves and ligated with two 3-0 sutures , while the left common carotid artery (LCCA) was ligated in the same way 1 week following right common carotid artery occlusion (RCCAO).MRI examinations were performed on a GE 3.0T MR scanner (Discovery 750, GE Healthcare, Milwaukee) using a HD wrist array. MRI techniques including three-dimensional arterial spin labelling perfusion imaging (3D ASL) and 3D time-of-flight magnetic resonance angiography (TOF-MRA) were used to detect dynamic changes in CBF and vertebral arteries (VAs).

Results and Discussion: It showed that the CBF of the cortex, basal ganglion and cerebellum dramatically decreased immediately after RCCAO, and remained reduced at 2 wk after BCCAO. However, it returned to the control level from 3 to 6 wk after BCCAO. In addition, the VA diameter gradually increased from 2 to 6 wk after BCCAO. Furthermore, CD34 immunofluorescence staining showed that the number of positive micro-vessels in these three areas was reduced at 2, 3 and 4 wk but increased at 6 wk after BCCAO. Our results suggest that CCH induces a compensation mechanism to maintain CBF in the brain s by dilation of VAs starting in the early stage and increases parallel with elevated angiogenesis in later stages.

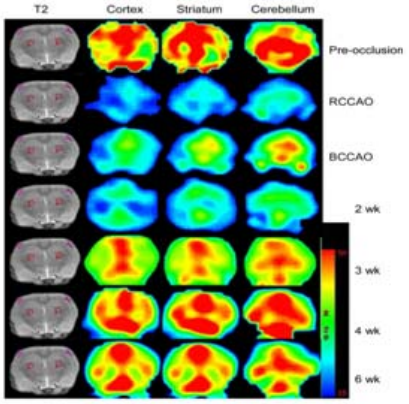

Fig.1

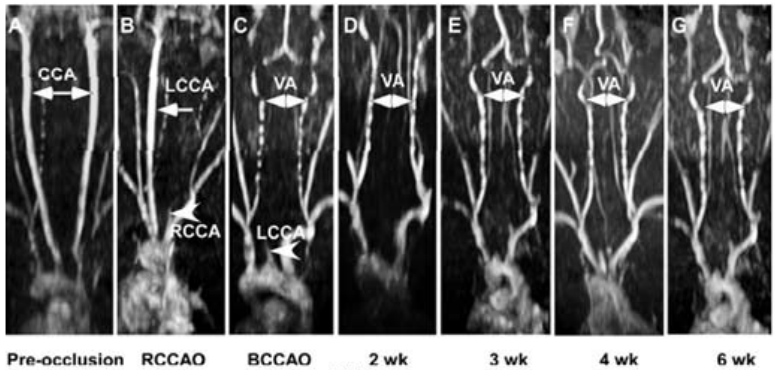

Fig.2

Figure 1. MRI images showing changes in CBF of the parietal cortex, basal ganglion and cerebellum at different time points after BCCAO. Areas in red in ASL images represent the strongest signal of CBF; and areas in blue or green reflect the weakest signal of CBF; and the yellow color is intermediate.**Figure 2. 3D TOF-MRA images showing morphological changes of CCAs and VAs in different groups.** In the pre-occlusion rats, the CCAs were clearly seen (A, arrows). After the RCCA was occluded, the RCCA signal disappeared (B, arrow head), but the LCCA was still visible (B, arrow). After BCCAO, both CCA signals were absent. At the same time, bead-like vertebral arties (VA) were seen (C, arrows). Gradual enlargement of VAs was observed from 2 wk to 6 wk after BCCAO (D, E, & F, arrows).

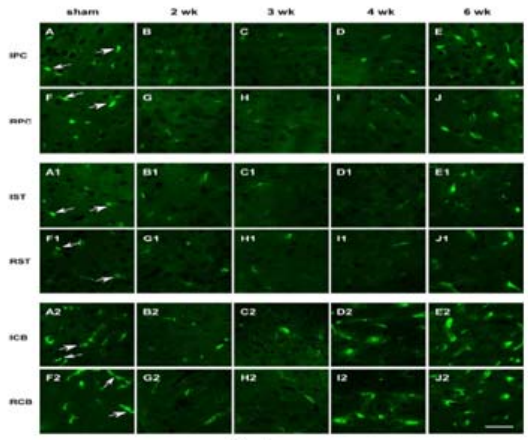

Fig.3

Figure3. Micrograph showing CD34 immunofluorescence staining in the parietal cortex, striatum and cerebellum. In the sham group, stronger staining of CD34 positive micro-vessels was seen in the parietal cortex (A & F, arrows), striatum (A1 & F1, arrows) and cerebellum (A2 & F2, arrows). However, the staining signal reduced at 2 wk (B, G, B1, G1, B2, G2), and 3 wk (C, H, 5C1, H1, 5C2, H2) in these three areas, and 4 wk (D, I, 5D1, I1) after BCCAO in the parietal cortex and the striatum. Stronger labeled CD34-positive micro-vessels reappeared earlier in the cerebellum at 4 wk (5D2, I2) and later at 6 wk (E, J, 5E1, J1, 5E2, J2) in the parietal cortex and the striatum after BCCAO. LPC, left parietal cortex; RPC, right parietal cortex; LST, left striatum; RST, right striatum; LCB, left cerebellum; RCB, right cerebellum. Scale bar, 20 μm.

References:

1.Jian H, Yi-Fang W, Qi L, Xiao-Song H, Gui-Yun Z. Cerebral blood flow and metabolic changes in hippocampal regions of a modified rat model with chronic cerebral hypoperfusion. Acta Neurol Belg. 2013 Sep;113(3):313-7.

2.Wong AM, Yan FX, Liu HL. Comparison of three-dimensional pseudo-continuous arterial spin labeling perfusion imaging with gradient-echo and spin-echo dynamic susceptibility contrast MRI. J Magn Reson Imaging. 2014 Feb;39(2):427-33.